Effect of double-diffusive convection with cross gradients on heat and mass transfer in a cubical enclosure with adiabatic cylindrical obstacles

Chakkingal, Manu; Voigt, Roland; Kleijn, Chris R.; Kenjereš, Saša

DOI
10.1016/j.ijheatfluidflow.2020.108574

Publication date
2020

Document Version
Final published version

Published in
International Journal of Heat and Fluid Flow

International Journal of Heat and Fluid Flow 83 (2020) 108574

Contents lists available at ScienceDirect

International Journal of Heat and Fluid Flow

journal homepage: www.elsevier.com/locate/ijhff

Effect of double-diffusive convection with cross gradients on heat and mass transfer in a cubical enclosure with adiabatic cylindrical obstacles

Manu Chakkingal[1,*], Roland Voigt[1], Chris R. Kleijn, Saša Kenjereš

Transport Phenomena Section, Department of Chemical Engineering, Delft University of Technology, Delft, The Netherlands

ARTICLE INFO

Keywords:
Natural convection
Double-diffusive convection
Temperature gradient
Concentration gradient
Obstacles
Quasi-steady flow
Laminar flow

ABSTRACT

We investigate natural convection driven by a horizontal temperature gradient and a vertical concentration gradient in fluid-filled enclosures with obstructions inside it. Within the domain, nine adiabatic and impermeable cylinders are placed, occupying 30% of the domain volume. The Boussinesq approximation is used to account for density variations within the fluid and the flow is fully resolved. The solutal Rayleigh number has been fixed at $Ra_C = 10^6$ and the Prandtl number at $Pr = 5.4$. The Lewis number has been varied in the range of $1 \leq Le \leq 100$ and the buoyancy ratio in the range of $0.1 \leq |N| \leq 10$. The rate of heat and mass transfer are compared to those found in single-scalar natural convection, i.e solely thermal or concentration driven convection. Besides, the obtained heat and mass transfer rate in the cylinder-packed enclosure have been compared to those found in a fluid-only domain. We observe that the addition of a destabilizing concentration gradient to a side-heated enclosure results in heat transfer enhancement, which decreases with Lewis number and thermal Rayleigh number. Similarly, the temperature gradient increases the mass transfer, especially at high Lewis numbers and lower concentration buoyancy force over its thermal counterpart. Although the presence of the cylindrical obstacles reduced the flow velocity, the mass transfer was enhanced at lower buoyancy ratio.

1. Introduction

When the density of a fluid is affected by both thermal and concentration gradients, the resulting natural convection flow in a gravity field is referred to as double diffusive convection, or two scalar natural convection, or combined natural convection heat and mass transfer. The existence of such a mechanism was first analysed in detail in 1956, when Stommel et al. described what they coined as an oceanographic curiosity (Stommel et al., 1956). It has become a topic of interest in oceanography (Huppert and Turner, 1981) ever since, as it is now commonly accepted to play a significant role in the vertical mixing of oceans (Radko, 2013).

Double diffusive convection is characterized by the solutal Rayleigh number Ra_C (which is a measure for the natural convection due to concentration gradients), the thermal Rayleigh number Ra_T (which is a measure for natural convection due to thermal gradients), the Schmidt number Sc (which is a measure for the diffusivity of the solute species in the fluid) and the Prandtl number Pr (which is a measure for the thermal conductivity of the fluid). The ratio Ra_c/Ra_T is referred to as the buoyancy ratio N, whereas the ratio Sc/Pr is referred to as the Lewis number Le. An important additional parameter is the mutual orientation between the directions of thermal and concentration gradients.

In addition to the interest in oceanography, the study of double diffusive convection has been picked up by scientists from other fields as well, due to its wide range of environmental and industrial applications, such as nuclear waste storage (Hao et al., 2017), magma chambers (Lowell, 1985), solar ponds (Akrour et al., 2011; Boudhiaf and Baccar, 2014), solidification of metals (Dong and Ebadian, 1995) as well as in stellar mixing (Canuto, 2010). In several of these applications, the flow is confined in complexly shaped enclosures, packed with solid internals. These packings can be seen as constituting a porous material that obstructs the flow. A detailed pore-scale study on such systems under forced convection is available in literature (Das et al., 2017; Buist et al., 2017; Das et al., 2018), but natural and double-diffusive convection in such geometries seems less investigated.

The particular application that is driving our research as described in this paper is molten iron production in the hearth of a blast furnace (Yang et al., 2016; Post et al., 2005). Here we are dealing with double diffusive convection due to perpendicular thermal and solutal gradients, viz. vertical concentration gradients between the top and bottom of the melt pool, and horizontal temperature gradients due to the

* Corresponding author.
E-mail address: M.Chakkingal@tudelft.nl (M. Chakkingal).
[1] M. Chakkingal and R. Voigt contributed equally to this manuscript.

https://doi.org/10.1016/j.ijheatfluidflow.2020.108574
Received 6 December 2019; Received in revised form 27 February 2020; Accepted 28 February 2020

Nomenclature

Ra_T	thermal Rayleigh number, $\frac{\mathbf{g}\beta_T(T_h - T_c)TL^3}{\nu\alpha}$
Ra_C	concentration Rayleigh number, $\frac{\mathbf{g}\beta_C(C_h - C_c)L^3}{\nu D}$
Nu	time- and wall- averaged Nusselt number, $\left\langle -\frac{L}{\Delta T}\left(\frac{\partial T}{\partial y}\right)\right\rangle_{\text{isothermal walls}}$
Sh	time- and wall- averaged Sherwood number, $\left\langle -\frac{L}{\Delta C}\left(\frac{\partial C}{\partial z}\right)\right\rangle_{\text{iso-concentration walls}}$
Pr	Prandtl number
δ	boundary layer thickness, m
Sc	Schmidt number
Le	Lewis number, $\frac{Sc}{Pr}$
N	buoyancy ratio, $\frac{\beta_C(C_h - C_c)}{\beta_T(T_h - T_c)}$
θ_T	non-dimensional temperature, $\frac{T - T_c}{T_h - T_c}$
θ_C	non-dimensional concentration, $\frac{C - C_c}{C_h - C_c}$
θ_ρ	non-dimensional density (for visualization), $\frac{\rho - \rho_{min}}{\rho_{max} - \rho_{min}}$
L	height of enclosure, m
$\mathbf{u}$	flow velocity, m/s
$\mathbf{u}^*$	non-dimensionalized velocity, $\frac{\mathbf{u}}{U_0}$
U_0	characteristic velocity scale, $\frac{Ra_T{}^{1/2}\alpha}{L}$, m/s
X, Y, Z	represents the rectangular coordinate system
g	accel. due to gravity (acts along Z axis), m/s^2
p	pressure, N/m^2
ρ	density of fluid, kg/m^3
ν	kinematic viscosity of fluid, m^2/s
β_T	coefficient of volume expansion of fluid due to temperature difference
β_C	solutal/concentration expansion factor
α	thermal diffusivity, m^2/s
D	concentration diffusivity, m^2/s
Re	Reynolds number based on root mean square velocity, $\frac{U_{rms}L}{\nu}$
U_{rms}	root mean square velocity averaged over time and volume, $\sqrt{<u_x^2 + u_y^2 + u_z^2>_{t,V}}$
δ_T^*	$\frac{\delta_T}{\text{Wall to cyl. distance}}$

Subscripts

h	high (when concentration), hot (when temperature)
c	low (when concentration), cold (when temperature)
T	temperature
C	concentration

cooling of the sidewalls. Furthermore, the large, unburnt coke particles in the hearth create a coarse grained porous packing, the length scales of which are comparable to those of the flow, thermal (Chakkingal et al., 2019; Ataei-Dadavi et al., 2019) and concentration fields. This plays an important role in the convection within the furnace and thus the power required to cool it. In order to understand and optimize flow and heat transfer in such systems, we need to understand double diffusive convection due to perpendicular density gradients, in an enclosure packed with coarse-grained obstructions. Such an insight is also relevant for other applications, such as determining the level of moisturization required to enhance flow in refrigeration systems (Laguerre et al., 2009) and to ensure safe storage of fuel close to heat sources (Bourich et al., 2004a).

A lot of studies have been published on (i) single scalar natural convection in porous materials and solid packings, on (ii) double diffusive convection with aligned temperature and concentration gradients in solid packings, and (iii) on double diffusive convection with perpendicular temperature and concentration gradients in fine-grained (extended-Darcy like) porous materials.

i. Many studies on convection in enclosures packed with solid objects addressed pure thermal convection only, i.e. convection due to density gradients as a result of thermal gradients only. An often studied situation is natural convection in a square enclosure with isothermal walls, and with single or multiple obstructions like cylinders and rods inside the enclosure. The position, thermal conductivity and size of the solid obstacles were found to have a large impact on the rate of heat transfer (Khanafer and Aithal, 2013; Alsabery et al., 2019; Braga and de Lemos, 2005) and flow (Yoon et al., 2009).
ii. Another group of studies addressed double diffusive convection with horizontal gradients of both temperature and concentration in fluid-only filled enclosures. Although already around the year 2000 Sezai and Mohamad (1999, 2000) performed 3D simulations and showed that such a flow is strictly three-dimensional for a wide range of parameters, most numerical investigations have been carried out in 2D. Corcione et al. (2015) provide an overview of several papers in such a setup. Correlations for Nu and Sh are presented for a wide parameter range. It was found that both heat and mass transfer increase as the thermal Rayleigh number and the Prandtl number are increased. Besides, it was noted that the mass transfer rate increases with the Lewis number. It was shown that the heat transfer rate is independent of Le number as long as the buoyancy ratio is lower than the value at which minimum heat transfer occurs, while it increases with Le if the buoyancy ratio is above this value. Double diffusive convection with horizontal gradients of both temperature and concentration in the presence of obstructing internals has received less attention in the literature. Laguerre et al. (2009) experimentally and numerically studied natural convection heat transfer of air in an enclosure filled with cylinders. It was found that moisturizing the bottom of the enclosure enhances the flow, i.e. higher velocities were measured in this case. Later, Xu et al. (2014) numerically studied double diffusive mixed convection in a square enclosure with inlet and outlet, in presence of an adiabatic cylinder of constant concentration. These authors analysed the effects of various governing parameters on the heat and mass transfer rates.
iii. Published studies on double diffusive convection in porous media filled enclosures with perpendicular gradients of temperature and concentration have been limited to fine grained porous media, that can be modelled with extended-Darcy type approaches. Mohamad and Bennacer (2001, 2002) numerically investigated 2D and 3D double diffusive natural convection with cross gradients using such a model. It was found that for the considered conditions, the difference in the rate of heat and mass transfer between two- and three-dimensional simulations is not significant, even though the flow shows a three-dimensional behaviour. Bourich et al. (2004b) presented an approach based on a scaling analysis to determine the order of magnitude of heat- and mass transfer in a square bottom-heated enclosure with horizontal concentration gradient, using the extended-Darcy model. The emphasis of this study was mostly on limiting cases of either dominating thermal or solutal buoyancy forces.

In conclusion, the existing literature does not provide insight in double diffusive convection due to perpendicular density gradients in an enclosure packed with large scale obstructions, as encountered in e.g. the hearth of blast furnaces, refrigeration systems, and fuel storage. Therefore, in the current work, we numerically study flow, heat and mass transfer in cross-gradient double diffusive convection in a cubical enclosure, with and without coarse grained obstructions. To better understand the influence of the large scale obstructions, we analyse local (i.e. pore scale) flow, temperatures and concentrations. We explain the influence of the cross-gradient on heat and mass transfer, and we provide new insights in the influence of large scale obstacles on local flow, heat and mass transfer.

2. Mathematical formulations and numerical methods

2.1. Physical problem

We analyze double-diffusive convection in two different domains, which are shown in Fig. 1. Both domains are cubic enclosures with sides L. The first domain is a fluid-only enclosure of volume L^3. In the second domain, 9 solid adiabatic cylinders are placed, holding a total volume of 30% of the domain. The cylinder radius, r can be calculated from $9\pi r^2 = (1-\epsilon)L^2$, where 9 represents the number of cylinders and $(1-\epsilon)$ is the solid fraction of the domain, resulting in $r/H \approx 0.1$. The details on the choice of location of cylinders are discussed later in Section 3.

The coordinate system is chosen such that gravity, $\mathbf{g}$ acts in the direction of the negative Z axis. No-slip condition is applied on every wall, including the surface area of the cylinders. The cylinders themselves are adiabatic and impermeable. The horizontal walls (top and bottom walls) are adiabatic and kept at a constant concentration C_h and C_c ($C_h > C_c$). The walls that are attached to the cylinders (front and back walls) are adiabatic and impermeable; and the other walls (left and right walls) are impermeable and maintained at isothermal temperatures T_h and T_c ($T_h > T_c$).

2.2. Governing equations and numerical schemes

In the simulations carried out we ensure that $|\beta_T \Delta T| < < 1$ and $|\beta_C \Delta C| < < 1$, so that Boussinesq's approximation is valid (Gray and Giorgini, 1976; Kizildag et al., 2014). This results in the simplified set of governing equations, constituting the continuity equation, Navier-Stokes equations, energy balance and species balance:

$$\frac{\partial u_i}{\partial x_i} = 0. \tag{1}$$

$$\frac{\partial u_i}{\partial t} + u_j \frac{\partial u_i}{\partial x_j} = -\frac{1}{\rho_o}\frac{\partial p}{\partial x_i} + \frac{\mu}{\rho_o}\frac{\partial^2 u_i}{\partial x_j^2} - g\frac{\rho(C,T)}{\rho_o}\delta_{i3}, \tag{2}$$

$$\frac{\partial T}{\partial t} = \alpha \frac{\partial^2 T}{\partial x_j^2} - u_j \frac{\partial T}{\partial x_j}, \tag{3}$$

$$\frac{\partial C}{\partial t} = D \frac{\partial^2 C}{\partial x_j^2} - u_j \frac{\partial C}{\partial x_j}. \tag{4}$$

Here, p, μ, δ_{i3}, ρ_o and $\rho(C, T)$ are the pressure, dynamic viscosity, Kronecker delta, reference density and the equation of state, respectively. The latter is expressed as a function of temperature and concentration as by the Boussinesq approximation, such that

$$\rho(C,T) = \rho_o[1 - \beta_T(T - T_0) - \beta_C(C - C_0)], \tag{5}$$

where T_0 and C_0 are the reference temperature and concentration that correspond to ρ_0, respectively.

Simulations were performed using a solver developed in FOAM-Extend 4.0, which is a fork of the OpenFOAM open source library for Computational Fluid Dynamics. The openFOAM solver, `buoyantBoussinesqPisoFoam`, is modified to solve two scalar equations, the validation of which is discussed in Appendix A. The numerical schemes available in FOAM-Extend, used for the simulations are listed in Table 1. The time derivatives are discretized by a second order implicit scheme. The Gauss entry in the gradient, divergence and Laplacian schemes refers to the fact that a standard finite volume approach is used. Gradients are calculated using a linear (central differencing) scheme. The divergence is calculated using a limited linear scheme to ensure stability and the Laplacian terms are found by a corrected linear scheme. The scheme entered for interpolation refers to the cell to face interpolation of values, ensuring conservation of mass.

The discretized governing equations were solved using the PISO algorithm. The time step for each simulation is calculated based on Courant-Friedrichs-Lewy (CFL) condition using adaptive time-stepping. In the present study, the time step was determined such that the Courant number was kept below 0.35.

2.3. Mesh requirement calculation

In order to estimate the required resolution in the boundary layer, correlations provided by (Shishkina et al., 2010) were utilized. Although these correlations were setup for turbulent (single scalar) Rayleigh-Bénard (RB) convection in a fluid-only domain, a reasonable estimate of the boundary layer thickness and corresponding required grid resolution could be made for both geometries. In order to be sure that the used resolution is fine enough to capture all the physics, a mesh dependency study was done for both geometries and all Lewis numbers, which is extensively discussed in Appendix B. The fluid-only domain is meshed using structured hexahedral cells, while locally structured cells (Fig. 2) are used for the cylinder-packed domain. Convergence of Nusselt number and Sherwood number (difference less than 0.5%), and comparison of plane-averaged temperature and concentration is used to ensure that the solutions are mesh independent. From the grid refinement study it is concluded that a mesh containing 2.1 million cells will be sufficient for the fluid-only domain. For the cylinder-packed domain, it was found that the required resolution is already achieved at 1.3 million cells. However, a finer mesh containing 3.8 million control volumes is used in the current simulations. We also ensure that there are at least 8 cells within the thermal and concentration boundary layers. We use the same refinement as that in the boundary layers, at the cylindrical surfaces.

3. Results and discussion

In order to be able to critically analyze the obtained results in the double-diffusive regime, the reference situations have to be understood. At first we discuss convection due to single scalar gradient; horizontal

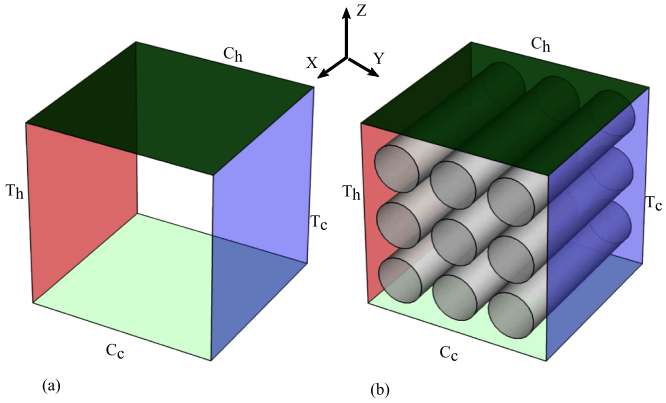

Fig. 1. Schematic representation of (a) fluid-only filled enclosure (b) enclosure with adiabatic cylindrical obstructions, with gravitational force along the negative Z direction.

Table 1
Numerical schemes.

Term	Scheme
Time derivative	Backward
Gradient	Gauss Linear
Divergence	Gauss Limited Linear 1
Laplacian	Gauss Linear Corrected
Interpolation	Linear

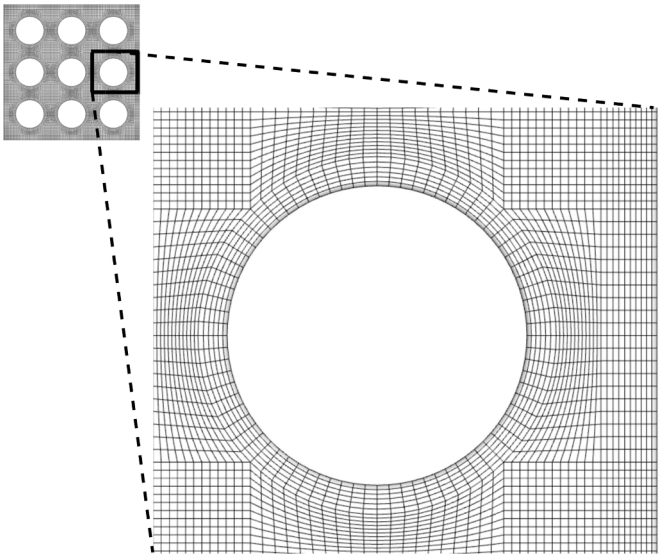

Fig. 2. Snapshot of front view of mesh for cylinder-packed enclosure, containing 3.8 million locally structured hexahedral cells.

temperature gradient (Section 3.1.1) at a fixed Prandtl number $Pr = 5.4$ and different thermal Rayleigh numbers Ra_T, followed by vertical concentration gradient (Section 3.1.2), for both fluid-only and cylinder-packed enclosure. Then, we discuss the double-diffusive convection due to the combined effect of both the scalars in Section 3.2.

The double-diffusive convection investigation is carried out at a fixed concentration Rayleigh number, $Ra_C = 10^6$ and at different Lewis number, Le. The Lewis number ($Le = Sh/Pr$) is varied from 1 to 100 by varying the Schmidt number in the range, $5.4 \leq Sc \leq 540$, while keeping the $Pr = 5.4$ constant. The cylinders are placed such that they are outside the concentration boundary layer $\left(\delta_C = \frac{L}{2Sh_0}\right)$ (Ng et al., 2015), while it is within the thermal boundary layer at low Ra_T $\left(\delta_T = \frac{L}{2Nu_0}\right)$ (Ng et al., 2015), where Sh_0 and Nu_0 are the Sherwood number and Nusselt number obtained in a fluid-only enclosure with only vertical concentration gradient (Section 3.1.2) and only horizontal temperature gradient (Section 3.1.1) respectively. All the results are expressed in non-dimensional form. Refer to the nomenclature for all the symbols and definitions.

3.1. Natural convection due to single scalar

The flow and heat/mass transfer characteristics obtained in single scalar natural convection are presented in this section. The considered parameters, used solver, geometry and numerical schemes are all identical to those used for two scalar natural convection. Pure thermal or solutal convection can be assured by simply setting β_C or β_T to zero.

3.1.1. Natural convection due to horizontal temperature gradient

The presence of cylinders in differentially heated enclosures, with no influence of concentration gradient ($\beta_C = 0$), suppress the time- and wall- averaged Nusselt number (Fig. 3) at low Ra_T. This suppression effect decreases as Ra_T increases. Unlike the fluid-only domain, the Nusselt number for pure conduction is lower than 1 for the cylinder-packed enclosure ($Nu = 0.55$) as the volume occupied by cylinders hinder conduction. As discussed in (Chakkingal et al., 2019; Ataei-Dadavi et al., 2019), the suppression of fluid flow by the obstructions resulting in lower heat transfer, becomes less effective with the increase in Ra_T due to the thinning of thermal boundary layer. Consequently, with the increase in Ra_T, the heat transfer in the enclosure with cylinders asymptotically approaches the heat transfer in a fluid-only filled enclosure (Lankhorst, 1991).

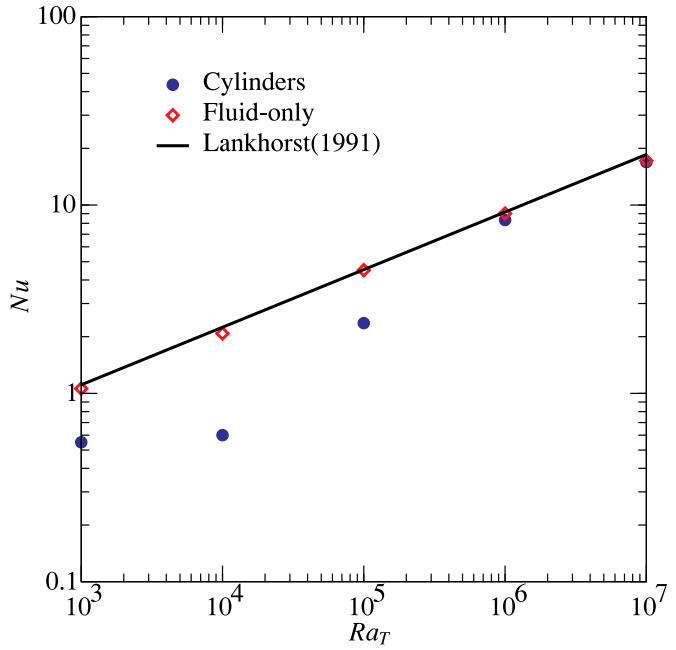

Fig. 3. Time- and wall- averaged Nusselt number Nu versus Ra_T for a side-heated enclosure at $Pr = 5.4$. Data obtained in the current study in fluid-only and cylinder-packed enclosures are plotted along with the $Nu = 0.136Ra_T^{0.305}$ scaling obtained for lateral heating of fluid-only filled cubic enclosure (Lankhorst, 1991).

The thickness of thermal boundary layer, δ_T calculated as in (Ng et al., 2015) $\left(\sim\frac{L}{2Nu}\right)$, is higher in an enclosure with cylinders than in a fluid-only enclosure, when the cylinders are placed within the thermal boundary layer. To understand the influence of cylinders we calculate the relative thickness of the thermal boundary layer when compared to the spacing between the vertical wall and the first column of cylinders:

$$\delta_T^* = \frac{\delta_T}{\text{Wall to cyl. distance}} \tag{6}$$

We also scale the thermal boundary layer thickness of a fluid-only filled enclosure with the wall to cylinder distance and check the influence of this ratio in enclosure with cylinders. From Fig. 4, we observe that the relative thickness of the thermal boundary layer of a fluid-only enclosure is higher than the cylinder to wall spacing (δ_T^* of fluid-only enclosure greater than 1), at low Ra_T. It indicates that the thermal boundary layer would be disturbed when the cylinders are placed (at this wall to cylinder distance) in a fluid-only enclosure at low Ra_T. We observe the thickening of the thermal boundary layer in enclosure with cylinders when they are placed within the thermal boundary layer of the fluid-only filled enclosure. Meanwhile, when the relative thickness δ_T^* of a fluid-only filled enclosure is less than 1 ($Ra_T > 10^6$), the thermal boundary layer thickness in enclosure with cylinders are unaffected, as the heat transfer becomes independent of the cylinders when they are placed outside a distance equal to the thermal boundary layer thickness

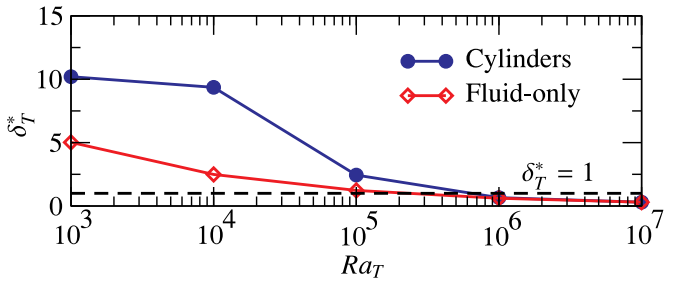

Fig. 4. Variation of thermal boundary layer thickness scaled with distance of the vertical wall from the first column of cylinders in fluid-only and cylinder-packed enclosure at different Ra_T. The black dotted line indicates the thickness of thermal boundary layer comparable to the cylinder to wall spacing.

of a fluid-only enclosure.

3.1.2. Solutal RB convection

In enclosures (with and without cylinders) with vertical concentration gradient at a fixed concentration Rayleigh number $Ra_C = 10^6$, we investigate the influence of Schmidt number ($5.4 \leq Sc \leq 540$). The presence of cylinders results in a steady state flow field, unlike the fluid-only domain where we obtain a transient flow at $Sc = 5.4$ and $Sc = 54$, and a steady flow at $Sc = 540$. However, the mass transfer (Sherwood number, Sh) is not influenced by the change in Sc (Fig. 5(a)).

Analogous to heat transfer (Grossmann and Lohse, 2001), for moderate to high Schmidt numbers ($Sc \gtrsim 1$), the mass transfer becomes practically independent of Sc. At a fixed Sc, mass transfer in enclosure with cylinders is higher than that in fluid-only enclosures, while the volume and time averaged Reynolds number, Re in enclosure with cylinders is lower. Though the Reynolds number at a fixed Sc in enclosure with cylinders is lower than in fluid-only filled enclosure (Fig. 5(b)), the cylinders modify the 3D-diagonal dominant flow in fluid-only enclosure (Valencia et al., 2007) to a pseudo 2D flow (Fig. 6). The flow in the out of plane direction (Y-Z plane) in a vertical plane becomes negligible in enclosure with cylinders, when compared to that in fluid-only enclosure. However, the convective heat transfer is slightly enhanced in enclosure with cylinders, with multiple rolls of fluid flow extending from the bottom to the top.

Increasing Sc results in a thinner concentration boundary layer, and therefore an enhancement in mass transfer might be expected. However, at constant Ra_C, an increase in Sc leads to a decrease in Grashof, (since $Ra_C = GrSc$) and hence, the applied buoyancy force

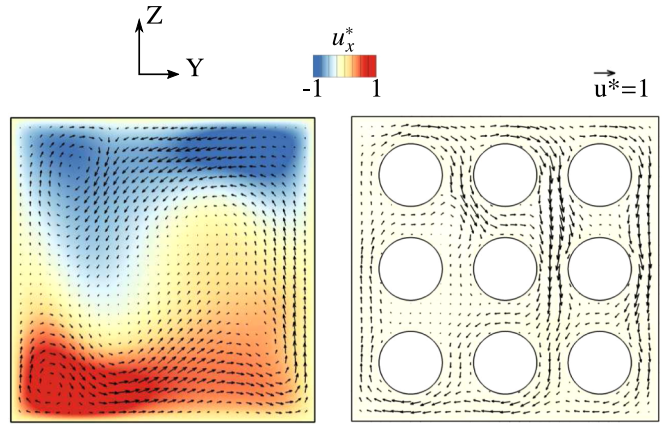

Fig. 6. Instantaneous non-dimensional out of plane velocity contour and in-plane velocity vectors at cross section $x/H = 0.5$ in (a) fluid-only (b) cylinder-packed enclosure, at $Ra_C = 10^6$, $Sc = 5.4$ for solutal RB convection.

decreases. Thus the higher Schmidt numbers do not necessarily lead to higher mass transfer rates. Although the mass transfer rate is practically independent of the Schmidt number in this configuration, the flow is not. Lower Schmidt numbers result in higher Reynolds numbers. The obtained Reynolds number at fixed Ra_C and varying Sc (Fig. 5(b)) for both the geometries follow a $Re \sim Sc^{-1}$ scaling for the considered parameter range, analogous to that in heat transfer (Grossmann and Lohse, 2002; Shishkina, 2016; Shishkina and Wagner, 2016).

3.2. Double diffusion due to temperature and concentration gradient

The combined effect of horizontal temperature gradient and vertical concentration gradient is analysed in this section. The relative strength of thermal diffusivity over mass diffusivity is expressed in terms of Lewis number $Le = \frac{Sc}{Pr}$, and the relative strength of solutal buoyant force over thermal buoyant force is expressed in terms of buoyancy ratio $N = \frac{\beta_C \Delta C}{\beta_T \Delta T}$. The concentration expansion factor, $\beta_C < 0$ (higher concentration leading to a denser fluid), resulting in a negative buoyancy ratio. In all our discussions below we use absolute value of buoyancy ratio, N.

The combined effect is analyzed at $Ra_C = 10^6$ and $Pr = 5.4$ at different Lewis number ($Le = 1 - 100$) and buoyancy ratio ($|N| = 0.1 - 10$). Unlike the solutal convection that generates flow patterns similar to those in Rayleigh-Bénard convection, the presence of

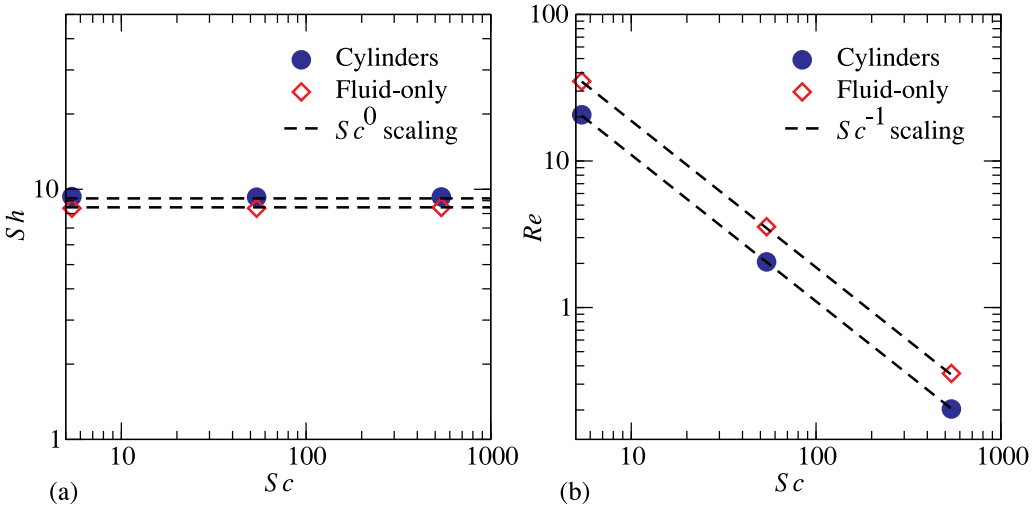

Fig. 5. (a) Sh versus Sc and (b) Re versus Sc in confined solutal RB convection at $Ra_C = 10^6$ for fluid-only and cylinder-packed enclosures.

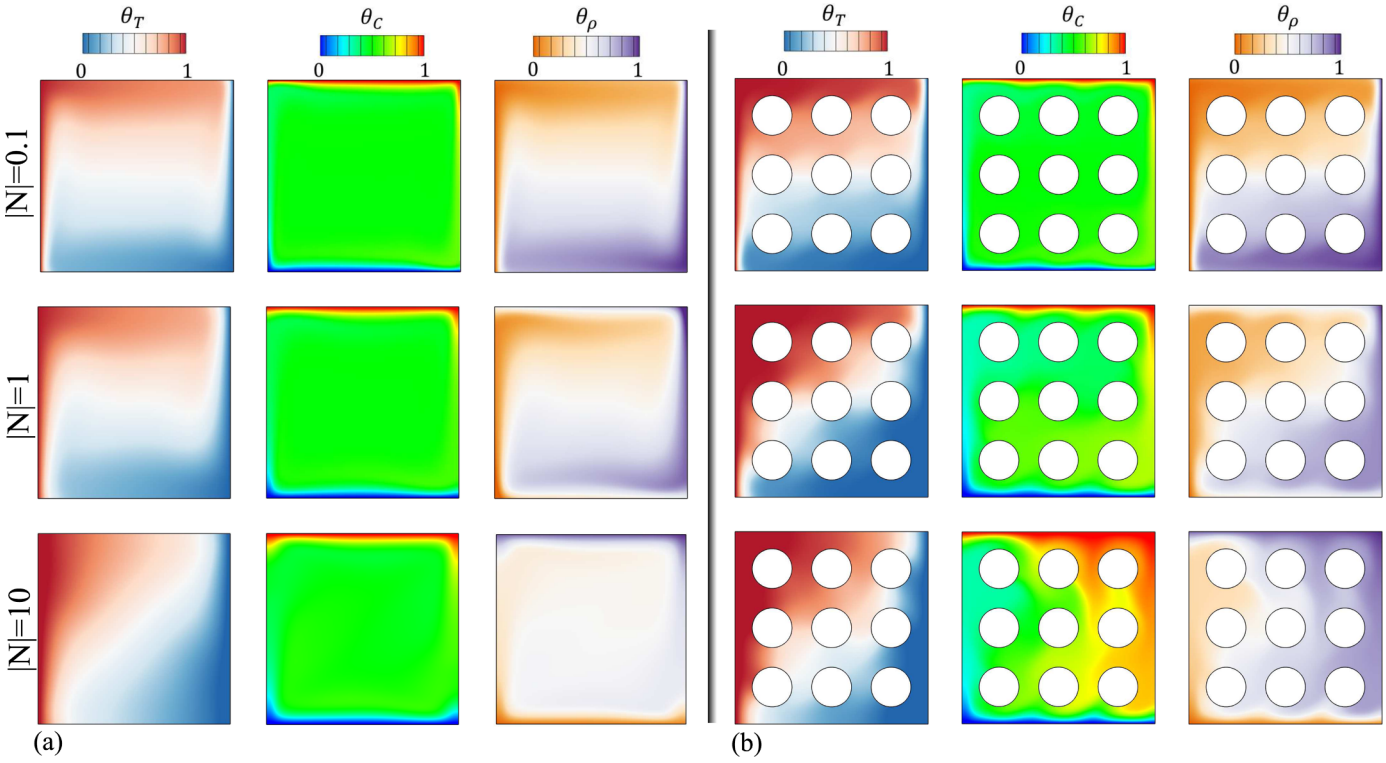

Fig. 7. Instantaneous contours of temperature, concentration and density at cross section $x/H = 0.5$ for $Ra_C = 10^6$, $Pr = 5.4$, $Le = 10$ and different values of $|N| = \frac{|\beta_C \Delta C|}{|\beta_T \Delta T|}$ in (a) fluid-only (b) cylinder-packed enclosures.

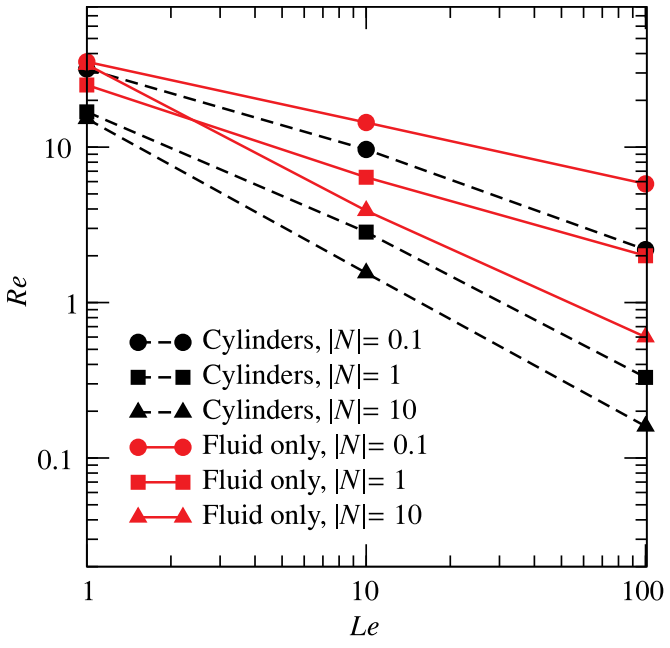

Fig. 8. *Re* versus *Le* at $Ra_C = 10^6$, and different $|N|$. Each point on the graph represents a simulation, while the lines in between serve to lead the eye.

an additional temperature gradient imposes a preferentially clock-wise oriented flow in both enclosures. In both enclosures (with and without cylinders), the effect of $|N|$ (Fig. 7) shows density variation similar to the temperature profile at $|N| = 0.1$, while at $|N| = 10$ it is similar to the concentration profile. The combined effect of equally strong temperature and concentration gradient, $|N| = 1$ results in a significantly different density distribution, that finally generates distinctive flow patterns. The cylindrical obstructions also influence the concentration and density distributions with the increase in buoyancy ratio ($|N| = 1, 10$). Unlike at $|N| = 0.1$, the flow is influenced by the obstruction, thus penetrating into the core of the enclosure before impinging the hot or the cold wall. The flow becomes three-dimensional at a higher buoyancy ratio for both configurations. Similar to the volume- and time- averaged *Re* in solutal RB convection (Fig. 5(b)) the *Re* in double diffusion (Fig. 8) at a fixed $|N|$ decreases with an increase in *Le*, both in fluid-only and cylinder-packed enclosures. The comparatively stronger flow at $Le = 1$ enhances the heat transfer (when compared to enclosure with temperature gradient alone) from the side walls at low $Ra_T = \frac{Ra_C}{|N|\,Le} = 10^5$ especially in the cylinder packed enclosure (Fig. 9). At the same *Le*, with a decrease in $|N|$ ($Ra_T = \frac{Ra_C}{|N|\,Le} = 10^6$) heat transfer enhances in enclosure with cylinders while that in the fluid-only enclosure becomes comparable to the heat transfer in a differentially heated enclosure with no mass transfer. With further decrease in $|N|$ ($Ra_T = \frac{Ra_C}{|N|\,Le} = 10^7$) the heat transfer in both the cavities with and without mass transfer, become comparable. At high $Le = 10$, the lower *Re* results in a weaker influence of the vertical concentration gradient on heat transfer, at low Ra_T. Thus at $Le = 10$, $Ra_T = \frac{Ra_C}{|N|\,Le} = 10^5$, the heat transfer enhancement in fluid-only and cylinder-packed (Fig. 9) enclosures with double-diffusion (red and black circles respectively) is lower than the respective cavities (red and black circles respectively) at $Le = 1$ and $Ra_T = 10^5$. Unlike at $Le = 1$, no enhancement in heat transfer is observed in cylinder-packed enclosure at $Ra_T = 10^6$ and $Le = 10$, when compared to a similar enclosure with temperature gradient alone. A reduction in *Re* with increase in *Le* results in this behaviour. With further increase in *Le* ($Le = 100$) at all Ra_T, the influence of the convective flow induced by the vertical solutal gradient becomes really low (due to low *Re*), resulting in heat transfer comparable to that in cavities with no mass transfer (horizontal temperature gradient alone).

In Fig. 9 at $Le = 1$ and $Ra_T = \frac{Ra_C}{|N|\,Le} = 10^5$ and enclosures with

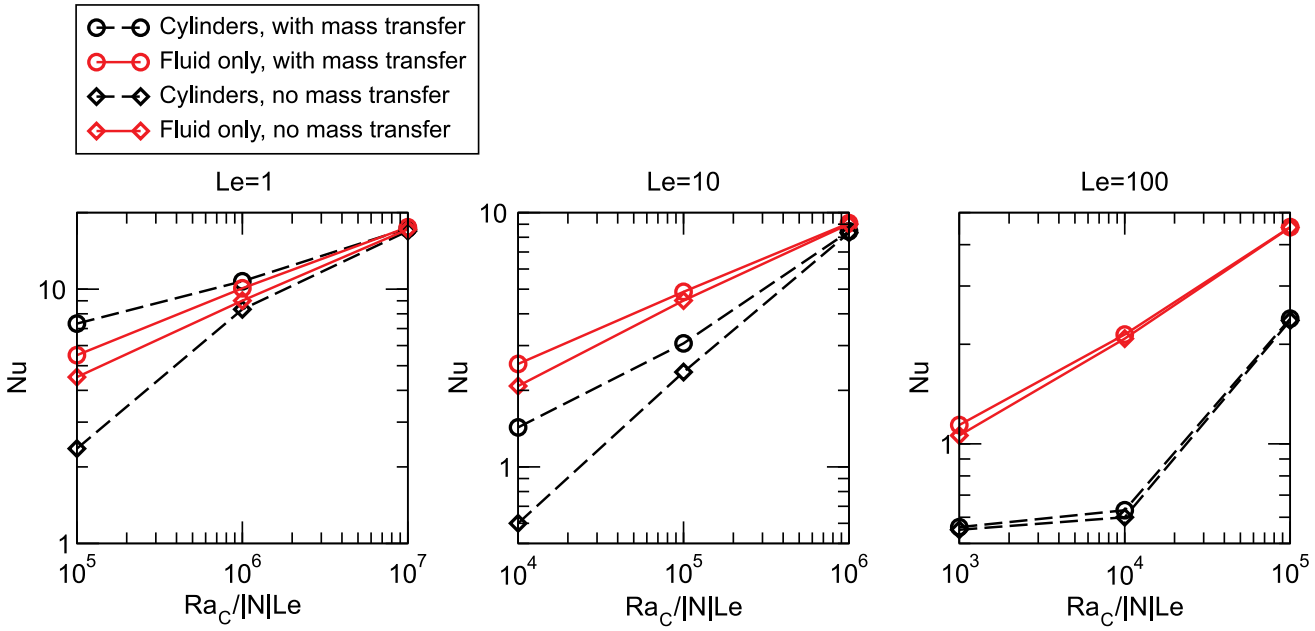

Fig. 9. Time- and wall- averaged Nusselt number *Nu*, as a function of $Ra_C/|N|Le$. Simulations with double diffusion have $Ra_C = 10^6$, $Pr = 5.4$ and different $|N|Le$. For simulations with temperature gradient alone, $Ra_C/|N|Le = Ra_T$ and $Pr = 5.4$. Each point again corresponds to a simulation, while the lines in between them serves to lead the eye.

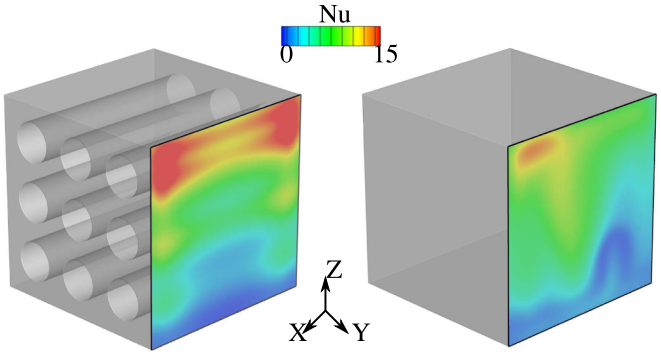

Fig. 10. Time- and wall- averaged Nusselt number *Nu*, for $Ra_C = 10^6$, $Pr = 5.4$, $Le = 1$ and $|N| = 10$ in enclosure with and without cylinders.

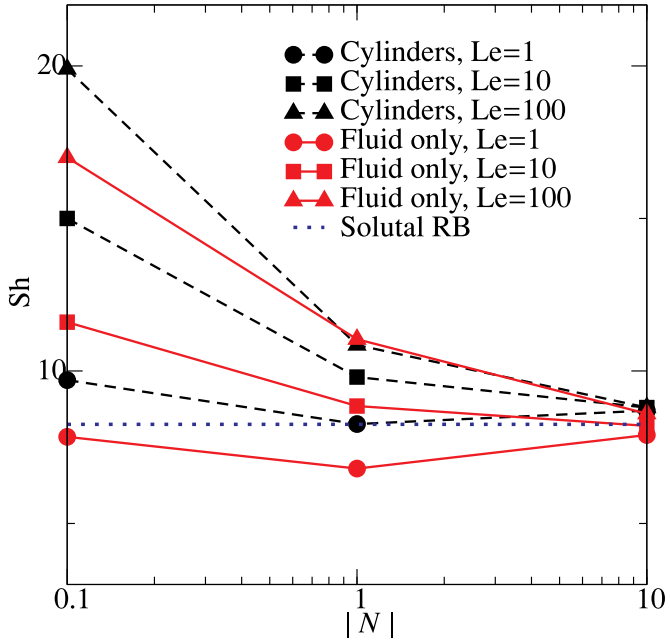

Fig. 11. Time- and wall- averaged Sherwood number *Sh* versus buoyancy ratio $|N|$ for $Ra_C = 10^6$, $Pr = 5.4$ and different *Le*. Each point on the graph represents a simulation, while the lines in between serve to lead the eye. The horizontal dotted line indicates the *Sh* in cylinder-packed cavity with no temperature gradient.

double diffusion, we also observe that the heat transfer in the enclosure with cylinders (black circle) is higher than in fluid-only enclosure (red circle). The cylinder-packed enclosure has a preferential clockwise direction of flow, whereas this flow pattern is absent in the fluid-only enclosure. In enclosure with cylinders the fluid at high concentration close to the top wall is directed to the right cold wall, and also penetrates to the center of the enclosure thus driving a portion of hot fluid along with it to the core of the enclosure. The imprint of such a flow can be easily seen in the local instantaneous Nusselt number distribution at the vertical wall (Fig. 10). A clockwise flow in the cylinder-packed enclosure results in most of the hot fluid to impinge at the top of the cold wall resulting in maximum heat transfer at the top, in contrast to the fluid-only enclosure in which a comparatively colder fluid impinges the cold wall over a wide area resulting in lower heat transfer.

The effect of double diffusion is more prominent in mass transfer, both in fluid-only and cylinder-packed enclosures (Fig. 11). Unlike solutal RB convection (Fig. 5(a)) the non-dimensional mass transfer is found to be very sensitive to changes in *Sc* (Fig. 11). This effect varies with $|N|$ (buoyancy ratio) and *Le* (equivalent to variation in *Sc* as *Pr* is fixed constant). Though the Reynolds number decreases with the increase in Lewis number, a significant increase in Sherwood number with Lewis number is observed at low buoyancy ratio. This mass transfer enhancement is not observed for higher buoyancy ratio $|N|$. At $|N| = 0.1$, the fluid density is mostly affected by the temperature resulting in a rotational flow, at a *Re* (Fig. 8) higher than in solutal RB convection Fig. 5(b)) at the same *Sc* ($Pr = 5.4$ being constant, change in *Le* is equivalent to change in *Sc*). Due to this rotational flow, the Lewis number becomes more important, as it is in forced convection (Schlichting, 2017; Janssen and Warmoeskerken, 2006).

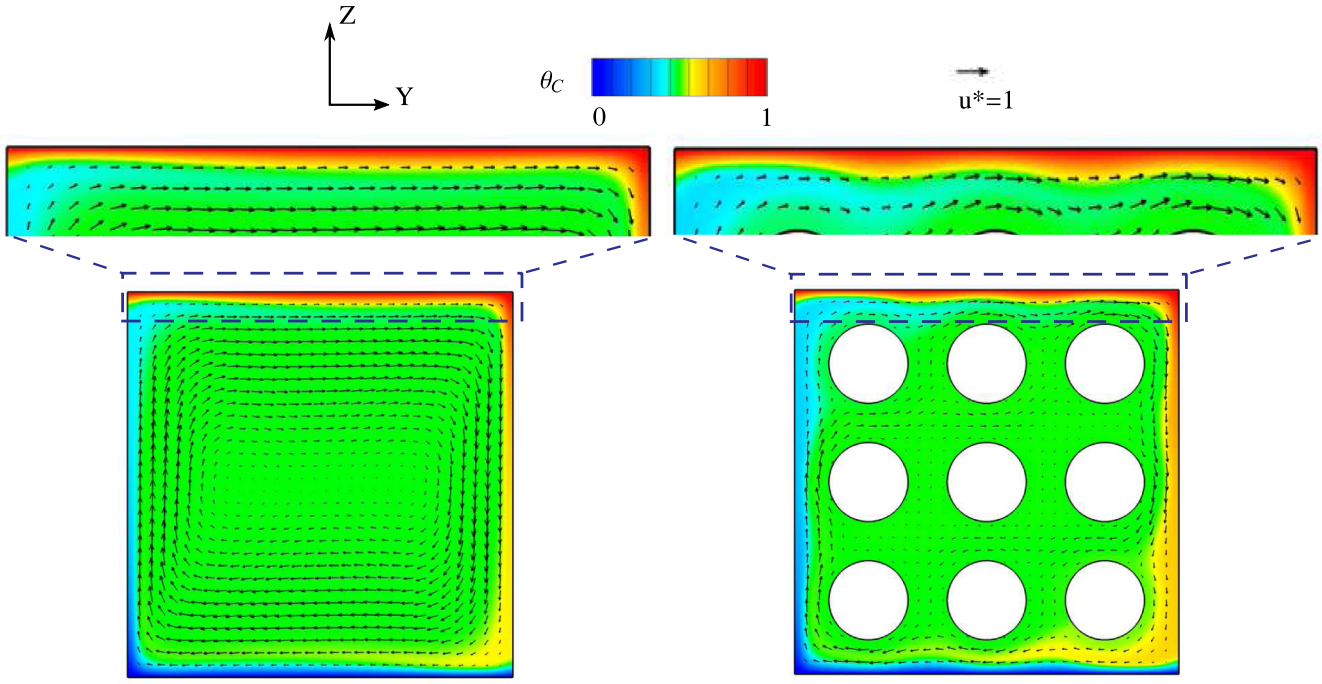

Fig. 12. Instantaneous concentration profile and velocity vectors at cross section $x/H = 0.5$ in (a) fluid-only (b) cylinder-packed enclosure, at $Ra_C = 10^6$, $Le = 100$ and $|N| = 0.1$.

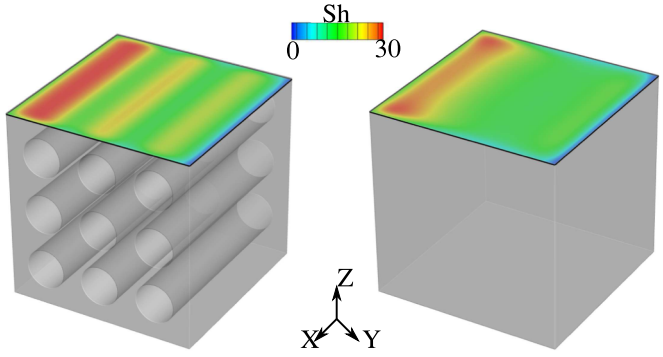

Fig. 13. Instantaneous local Sherwood numbers at top plane for $Ra_C = 10^6$, $Pr = 5.4$, $Le = 100$ and $|N| = 0.1$.

The obtained Sherwood numbers show that, in general, higher mass transfer is achieved in the cylinder-packed domain as compared to the fluid-only domain, with maximum enhancement at low $|N|$. Fig. 12 shows the contours of concentration and velocity vectors at $|N| = 0.1$, $Le = 100$ for both enclosures. Unlike the fluid-only enclosure, fluid above the cylinders close to the top wall though at lower flow velocity, are of comparatively lower concentration. The flow in the cylinder-packed enclosure is not strictly parallel to the top wall as in fluid-only enclosure, but is pushed towards the top wall resulting in a higher mass transfer (Fig. 13). This distribution is generated by the directional flow resulting from the blockage effects of the cylinders.

4. Summary and conclusion

A detailed study on the effect of horizontal temperature gradient, vertical concentration gradient and their combined effect under different diffusive strength Le and buoyancy ratio $|N|$ is carried out, in fluid-filled enclosures with and without obstacles. Major findings are summarized as follows:

i. The heat transfer in enclosures with horizontal temperature gradient alone is/ is not influenced by the obstacles depending on their location w.r.t to the thermal boundary layer. Presence of obstacles within the thermal boundary layer results in suppression of heat transfer, whereas the heat transfer is similar to that in fluid-only enclosures when the obstacles are outside the thermal boundary layer.
ii. Similar to fluid-only enclosures, although the Reynolds number decreases with the increase in Sc ($Re \sim Sc^{-1}$), mass transfer in cylinder-packed enclosures with vertical concentration gradient is practically not affected by the change in Sc ($Sh \sim Sc^{0}$). Modification of the flow field by the cylinders results in mass transfer close to that in fluid-only enclosures, despite the fact that the average Reynolds number is lower in the former.
iii. The combined effect of cross gradients in double-diffusive convection results in enhancement in heat transfer at lower thermal Rayleigh numbers, with considerable influence of cylinders at lower Lewis number and higher buoyancy ratio. With an increase in Lewis number, the heat transfer becomes independent of the vertical concentration gradient. Similar to an enclosure with horizontal temperature gradient alone, the heat transfer in both the enclosures approach each other with the increase in thermal Rayleigh number.
iv. In both configurations with double diffusion, at lower buoyancy ratio, the mass transfer at the horizontal walls are highly enhanced (increase by more than 100% at $Le = 100$, $|N| = 0.1$) with the increase in Lewis number, unlike the enclosures with concentration gradient alone. The modification of flow and the concentration distribution by the cylinders results in higher mass transfer compared to fluid-only enclosures. The enhancement in mass transfer vanishes with the increase in buoyancy ratio and becomes comparable to enclosures with only concentration gradient.

The current study with a fixed number of cylinders helps us to understand the influence of disturbing the boundary layers with obstructions and its influence on flow and heat/mass transfer. We find that in enclosures with coarse-grained obstructions, the shape of obstruction close to the walls can modify the local flow and even result in an enhancement in mass transfer. We also find that when the pore-space is bigger than the thermal/solutal length scale, the heat transfer from the vertical walls is similar to fluid-only cavities with no mass transfer. We could thus make use of heat transfer-correlations for fluid-only enclosures neglecting the solutal effects at high thermal Rayleigh number operating conditions. We propose to study more complex packings like packed beds of different thermal properties to confirm the applicability of our findings.

CRediT authorship contribution statement

Manu Chakkingal: Conceptualization, Data curation, Formal analysis, Investigation, Methodology, Supervision, Validation, Visualization, Writing - original draft. **Roland Voigt:** Data curation, Formal analysis, Investigation, Methodology, Validation, Visualization, Writing - original draft. **Chris R. Kleijn:** Project administration, Resources, Funding acquisition, Supervision, Writing - review & editing. **Saša Kenjereš:** Project administration, Visualization, Software, Funding acquisition, Supervision, Writing - review & editing.

Declaration of Competing Interest

The authors declare that they have no known competing financial interests or personal relationships that could have appeared to influence the work reported in this paper.

Acknowledgments

This research was carried out under project number S41.5.14526a in the framework of the Partnership Program of the Materials innovation institute M2i (www.m2i.nl) and the Technology Foundation TTW (www.stw.nl), which is part of the Netherlands Organization for Scientific Research (www.nwo.nl). We would like to thank our industrial partner TATA Steel, The Netherlands, for continuous financial support and SURFsara for the support in using the Cartesius Computing Cluster (NWO File No. 175507128).

Appendix A. Solver validation

To validate the solver developed, we carried out 3D simulations in an empty enclosure with horizontal gradients of temperature and concentration; and compare the results with literature. No work has been found on three dimensional double-diffusive convection with cross gradients. However, (Sezai and Mohamad, 2000) provide obtained average Nusselt numbers for 3D simulations in an empty enclosure with horizontal gradients of temperature and concentration. For these simulations, they used a mesh with 80^3 control volumes with refinement near the walls. (Béghein et al., 1992) studied a similar system in 2D, using a mesh of 40 $\times$ 40 cells. The obtained average Nusselt numbers on a mesh of 128^3 cells are plotted for $Ra_T = 10^7$, $Pr = 0.71$, $Le = 1$ and different buoyancy ratios in Fig. A.14. The obtained results differ less than 1% from those by Sezai and Mohamad and less than 0.1% from those by Béghein et al. It can thus be concluded that the used solver is suitable for two scalar natural convection.

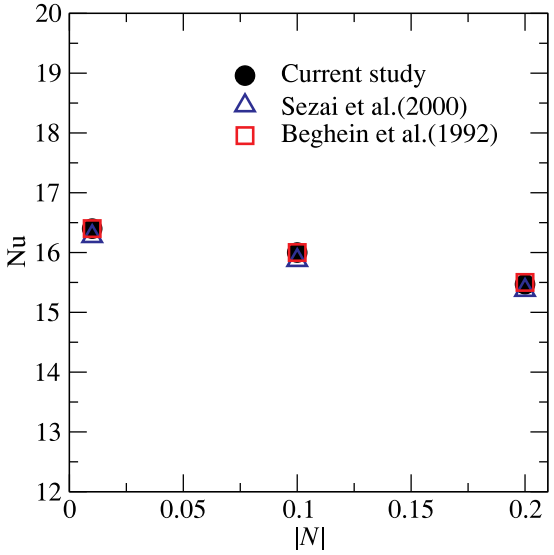

Fig. A1. Comparison of average Nusselt number for $Ra_T = 10^7$, $Pr = 0.71$, $Le = 1$ with results from literature (Sezai and Mohamad, 2000; Béghein et al., 1992).

Appendix B. Mesh independence study

A mesh validation study has been carried out for the geometries, at three different Lewis numbers. The time-averaged temperature and concentration are averaged along planes perpendicular to the temperature gradient and concentration gradients respectively in both fluid-only (Fig. B.16) and cylinder-packed (Fig. B.15) enclosures; and is plotted against the 3rd coordinate axis. With the chosen parameters, the highest thermal Rayleigh number occurs at $Le = 1$, making this a suitable case for a mesh dependency study. On the other hand, higher Lewis numbers lead to higher mass transfer rates, making the required resolution in the boundary layer a lot higher. Thus separate mesh refinement study is carried out for all three Lewis numbers, the results from $Le = 10$ being reported below with others available in supplementary material.

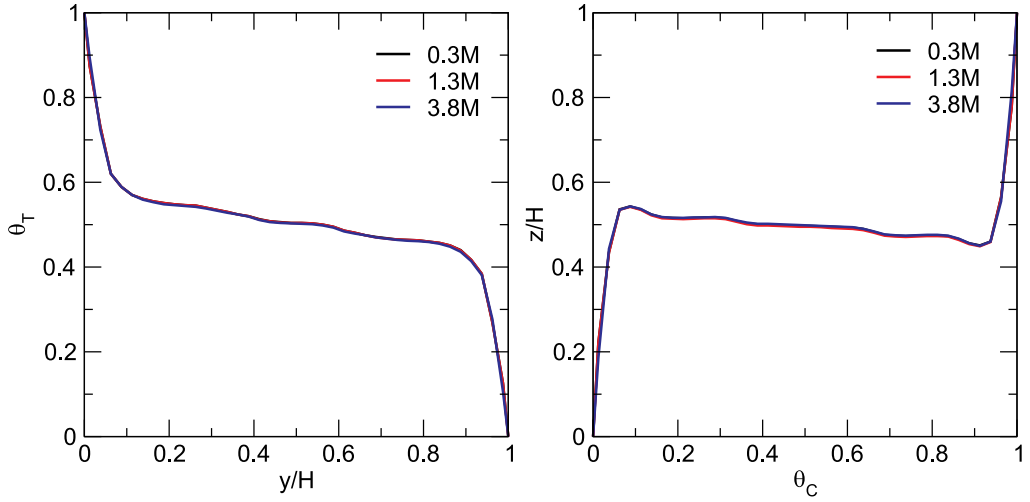

Fig. B1. Plane-averaged temperature and concentration profiles for $Ra_C = 10^6$, $Pr = 5.4$, $|N| = 0.1$, $Le = 10$ in a cylinder-packed enclosure, using 0.3 million, 1.3 million and 3.8 million cells.

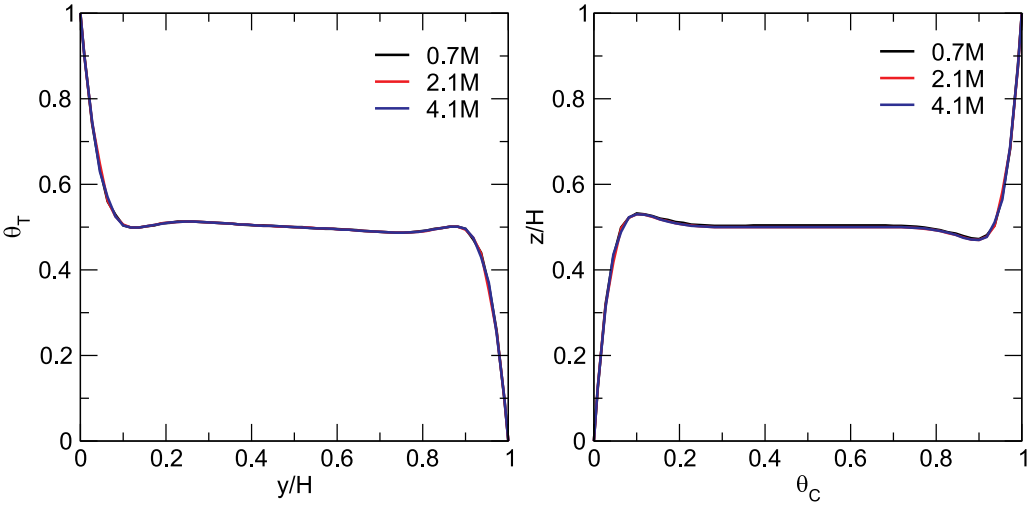

Fig. B2. Plane-averaged temperature and concentration profiles for $Ra_C = 10^6$, $Pr = 5.4$, $|N| = 0.1$, $Le = 10$ in a fluid-only filled enclosure, using 0.7 million, 2.1 million and 4.1 million cells.

Supplementary material

Supplementary material associated with this article can be found, in the online version, at 10.1016/j.ijheatfluidflow.2020.108574

References

Akrour, D., Tribeche, M., Kalache, D., 2011. A theoretical and numerical study of thermosolutal convection: stability of a salinity gradient solar pond. Therm. Sci. 15 (1), 67–80. https://doi.org/10.2298/tsci1101067a.

Alsabery, A.I., Mohebbi, R., Chamkha, A.J., Hashim, I., 2019. Effect of local thermal non-equilibrium model on natural convection in a nanofluid-filled wavy-walled porous cavity containing inner solid cylinder. Chem. Eng. Sci. 201, 247–263. https://doi.org/10.1016/j.ces.2019.03.006.

Ataei-Dadavi, I., Chakkingal, M., Kenjeres, S., Kleijn, C.R., Tummers, M.J., 2019. Flow and heat transfer measurements in natural convection in coarse-grained porous media. Int. J. Heat Mass Transf. 130, 575–584. https://doi.org/10.1016/j.ijheatmasstransfer.2018.10.118.

Béghein, C., Haghighat, F., Allard, F., 1992. Numerical study of double-diffusive natural convection in a square cavity. Technical Report.

Boudhiaf, R., Baccar, M., 2014. Transient hydrodynamic, heat and mass transfer in a salinity gradient solar pond: a numerical study. Energy Convers. Manag. 79, 568–580. https://doi.org/10.1016/j.enconman.2013.12.068.

Bourich, M., Hasnaoui, M., Amahmid, A., 2004. Double-diffusive natural convection in a porous enclosure partially heated from below and differentially salted. Int. J. Heat Fluid Flow 25 (6), 1034–1046. https://doi.org/10.1016/j.ijheatfluidflow.2004.01.003.

Bourich, M., Hasnaoui, M., Amahmid, A., 2004. A scale analysis of thermosolutal convection in a saturated porous enclosure submitted to vertical temperature and horizontal concentration gradients. Energy Convers. Manag. 45 (18-19), 2795–2811. https://doi.org/10.1016/j.enconman.2004.01.010.

Braga, E.J., de Lemos, M.J., 2005. Laminar natural convection in cavities filled with circular and square rods. Int. Commun. Heat Mass Transf. 32 (10), 1289–1297. https://doi.org/10.1016/j.icheatmasstransfer.2005.07.014.

Buist, K., Backx, B., Deen, N., Kuipers, J., 2017. A combined experimental and simulation study of fluid-particle heat transfer in dense arrays of stationary particles. Chem. Eng. Sci. 169, 310–320. https://doi.org/10.1016/j.ces.2016.04.022.

Canuto, V.M., 2010. Stellar mixing. Astron. Astrophys. 528, A76. https://doi.org/10.1051/0004-6361/201014447.

Chakkingal, M., Kenjereš, S., Ataei-Dadavi, I., Tummers, M., Kleijn, C.R., 2019. Numerical analysis of natural convection with conjugate heat transfer in coarse-grained porous media. Int. J. Heat Fluid Flow 77, 48–60. https://doi.org/10.1016/j.ijheatfluidflow.2019.03.008.

Corcione, M., Grignaffini, S., Quintino, A., 2015. Correlations for the double-diffusive natural convection in square enclosures induced by opposite temperature and concentration gradients. Int. J. Heat Mass Transf. 81, 811–819. https://doi.org/10.1016/j.ijheatmasstransfer.2014.11.013.

Das, S., Deen, N.G., Kuipers, J., 2017. A DNS study of flow and heat transfer through slender fixed-bed reactors randomly packed with spherical particles. Chem. Eng. Sci. 160, 1–19. https://doi.org/10.1016/j.ces.2016.11.008.

Das, S., Panda, A., Deen, N., Kuipers, J., 2018. A sharp-interface immersed boundary method to simulate convective and conjugate heat transfer through highly complex periodic porous structures. Chem. Eng. Sci. 191, 1–18. https://doi.org/10.1016/j.ces.2018.04.061.

Dong, Z., Ebadian, M., 1995. Numerical simulation of double diffusive convection in a v-shaped sump. Int. J. Heat Fluid Flow 16 (4), 236–243. https://doi.org/10.1016/0142-727x(95)00028-o.

Gray, D.D., Giorgini, A., 1976. The validity of the boussinesq approximation for liquids and gases. Int. J. Heat Mass Transf. 19 (5), 545–551. https://doi.org/10.1016/0017-9310(76)90168-X.

Grossmann, S., Lohse, D., 2001. Thermal convection for large Prandtl numbers. Phys. Rev. Lett. 86 (15), 3316–3319. https://doi.org/10.1103/PhysRevLett.86.3316.

Grossmann, S., Lohse, D., 2002. Prandtl and Rayleigh number dependence of the Reynolds number in turbulent thermal convection. Phys. Rev. E 66 (2002). https://doi.org/10.1103/physreve.66.016305.

Hao, Y., Nitao, J.J., Buscheck, T.A., Sun, Y., 2017. Double-diffusive natural convection in a nuclear waste repository. Nucl. Technol. 163 (1), 38–46. https://doi.org/10.13182/nt08-a3968.

Huppert, H.E., Turner, J.S., 1981. Double-diffusive convection. J. Fluid Mech. 106 (-1), 299. https://doi.org/10.1017/s0022112081001614.

Janssen, L., Warmoeskerken, M., 2006. Transport Phenomena Data Companion, fourth ed. VSSD, Delft.

Khanafer, K., Aithal, S.M., 2013. Laminar mixed convection flow and heat transfer characteristics in a lid driven cavity with a circular cylinder. Int. J. Heat Mass Transf. 66, 200–209. https://doi.org/10.1016/j.ijheatmasstransfer.2013.07.023.

Kizildag, D., Rodríguez, I., Oliva, A., Lehmkuhl, O., 2014. Limits of the Oberbeck Boussinesq approximation in a tall differentially heated cavity filled with water. Int. J. Heat Mass Transf. 68, 489–499. https://doi.org/10.1016/j.ijheatmasstransfer.2013.09.046.

Laguerre, O., Benamara, S., Remy, D., Flick, D., 2009. Experimental and numerical study of heat and moisture transfers by natural convection in a cavity filled with solid obstacles. Int. J. Heat Mass Transf. 52 (25-26), 5691–5700. https://doi.org/10.1016/j.ijheatmasstransfer.2009.07.028.

Lankhorst, A.M., 1991. Laminar and Turbulent Convection in Cavities: Numerical Modeling and Experimental Validation. Technische Univ., Delft (Netherlands). Ph.D. Thesis.

Lowell, R.P., 1985. Double-diffusive convection in partially molten silicate systems: its role during magma production and in magma chambers. Technical Report.

Mohamad, A., Bennacer, R., 2002. Double diffusion, natural convection in an enclosure filled with saturated porous medium subjected to cross gradients ; stably stratified fluid. Int. J. Heat Mass Transf. 45 (18), 3725–3740. https://doi.org/10.1016/s0017-9310(02)00093-5.

Mohamad, A.A., Bennacer, R., 2001. Natural convection in a confined saturated porous medium with horizontal temperature and vertical solutal gradients. Int. J. Therm. Sci. 40 (1), 82–93. https://doi.org/10.1016/s1290-0729(00)01182-0.

Ng, C.S., Ooi, A., Lohse, D., Chung, D., 2015. Vertical natural convection: application of the unifying theory of thermal convection. J. Fluid Mech. 764, 349–361. https://doi.org/10.1017/jfm.2014.712.

Post, J., Togarelli, D., van der Stel, J., Yang, Y., Reuter, M., 2005. Hot metal flow in the hearth of a blast furnace: influence of dynamic changes dead man porosity due to coke dissolution and coke size changes. Proc. 5th European Coke and Ironmaking Congress–5th ECIC, Stockholm, Sweden. pp. 1–16.

Radko, T., 2013. Double-Diffusive Convection, first ed. Cambridge University Press.

Schlichting, H., 2017. Boundary Layer Theory, ninth ed. Springer.

Sezai, I., Mohamad, A.A., 1999. Three-dimensional double-diffusive convection in a porous cubic enclosure due to opposing gradients of temperature and concentration. J. Fluid Mech. 400, 333–353. https://doi.org/10.1017/s0022112099006540.

Sezai, I., Mohamad, A.A., 2000. Double diffusive convection in a cubic enclosure with opposing temperature and concentration gradients. Phys. Fluids 12 (9), 2210–2223. https://doi.org/10.1063/1.1286422.

Shishkina, O., 2016. Momentum and heat transport scalings in laminar vertical convection. Phys. Rev. E 93 (2016). https://doi.org/10.1103/physreve.93.051102.

Shishkina, O., Stevens, R.J.A.M., Grossmann, S., Lohse, D., 2010. Boundary layer structure in turbulent thermal convection and its consequences for the required numerical resolution. New J. Phys. 12 (7), 075022. https://doi.org/10.1088/1367-2630/12/7/075022.

Shishkina, O., Wagner, S., 2016. Prandtl-number dependence of heat transport in laminar horizontal convection. Phys. Rev. Lett. 116 (2016). https://doi.org/10.1103/physrevlett.116.024302.

Stommel, H., Arons, A.B., Blanchard, D., 1956. An oceanographical curiosity: the perpetual salt fountain. Deep Sea Res. 3 (2), 152–153. https://doi.org/10.1016/0146-6313(56)90095-8.

Valencia, L., Pallares, J., Cuesta, I., Grau, F.X., 2007. Turbulent Rayleigh–Bénard convection of water in cubical cavities: a numerical and experimental study. Int. J. Heat Mass Transf. 50 (15–16), 3203–3215. https://doi.org/10.1016/j.ijheatmasstransfer.2007.01.013.

Xu, H., Wang, Z., Karimi, F., Yang, M., Zhang, Y., 2014. Numerical simulation of double diffusive mixed convection in an open enclosure with different cylinder locations. Int. Commun. Heat Mass Transf. 52, 33–45. https://doi.org/10.1016/j.icheatmasstransfer.2014.01.005.

Yang, W.-J., Mochizuki, S., Nishiwaki, N., 2016. Transport Phenomena in Manufacturing and Materials Processing. 6 Elsevier.

Yoon, H.S., Ha, M.Y., Kim, B.S., Yu, D.H., 2009. Effect of the position of a circular cylinder in a square enclosure on natural convection at Rayleigh number of 10^7. Phys. Fluids 21 (4), 47101. https://doi.org/10.1063/1.3112735.